Available online at www.sciencedirect.com
SCIENCE DIRECT®
Biochemical and Biophysical Research Communications 329 (2005) 495–501
BBRC
www.elsevier.com/locate/ybbrc

Cis/*trans* heterogeneity of Gln30-Pro31 peptide bond determines whether a 79-residue fragment of staphylococcal nuclease self-associates

Xu Wang, Yufeng Tong, Jinfeng Wang *

National Laboratory of Biomacromolecules, Center for Structural and Molecular Biology, Institute of Biophysics, Chinese Academy of Sciences, 15 Datun Road, Beijing 100101, China

Received 26 January 2005

Abstract

The self-association reaction of a 79-residue fragment of staphylococcal nuclease (SNase79) was studied by far-UV CD, size-exclusion chromatography, and heteronuclear multidimensional NMR spectroscopy. A large population of SNase79 is in self-associated state while a small population of SNase79 is essentially in a monomeric state. The sequence region Thr13-Val39 is responsible for association interface of SNase79. The *trans*-conformation of X-prolyl bond Gln30-Pro31 may make residues Tyr27-Gln30, serve as a folding nucleation site, and lead the segment Thr13-Val39 of SNase79 to adopt a native-like β-sheet conformation, which results in the self-association of SNase79. The non-native conformation of the segment Thr13-Val39 of SNase79 associated with the *cis*-conformation of X-prolyl bond Gln30-Pro31 may preclude SNase79 from the soluble aggregates.

Keywords: Self-association; *Cis*/*trans* heterogeneity; X-prolyl bond; Association interface; β-sheet conformation

Staphylococcal nuclease (SNase) (MW 17 kDa) contains a main hydrophobic core consisting of a β-sheet (βI) and a β-sheet (βII). The N-terminal 79-residue fragment of staphylococcal nuclease (SNase79) contains a complete β-sheet (βI) and an incomplete β-sheet (βII) region. In native SNase (Fig. 1), the β-sheet (βI) comprises three β-strands: strand β_1 (Thr13-Ala17); strand β_2 (Thr22-Met26); and strand β_3 (Pro31-Arg35), and two β-turns: τ_1 (Ile18-Asp21) and τ_2 (Tyr27-Gln30). Three β-strands: strand β_4 (His8-Ala12), strand β_5 (Ile72-Phe76), and strand β_6 (Ala90-Tyr93) construct the β-sheet (βII) for native SNase. The β-sheet (βI) and β-sheet (βII) form a "β-barrel" structural region in the native SNase [1]. Sequence of SNase79 does not fulfill a requirement for constructing the "β-barrel" structure. SNase79 can be regarded as a connecting link between SNase36 (36-residue SNase fragment) and SNase110 (110-residue SNase fragment). SNase36 contains all amino acid residues involved in the formation of β-sheet (βI) in the native SNase. SNase110 contains the sequence regions corresponding to the structural elements of native SNase: a "β-barrel" hydrophobic core, helices α_1 (Ala58-Ala69) and α_2 (Met98-Gln106), and loops ([omega]-loop: Pro42-Glu57; thymidine 3′,5′-bisphosphate (pdTp) binding loop: Asp77-Leu89; and C-terminal extension of helix α_2: Gly107-Lys110). Studies of SNase36 and other two N-terminal short fragments of SNase suggested that the nuclei for initiation folding of polypeptide chain are constructed transiently around the β-turn regions of SNase36, however the native-like β-sheet (βI) conformation cannot be observed for SNase36 [2]. The previous studies of SNase110 demonstrated that the residues 1–110 of SNase are necessary

* Corresponding author. Fax: +86 10 6487 2026.
E-mail address: jfw@sun5.ibp.ac.cn (J. Wang).

0006-291X/$ - see front matter © 2005 Elsevier Inc. All rights reserved.
doi:10.1016/j.bbrc.2005.01.155

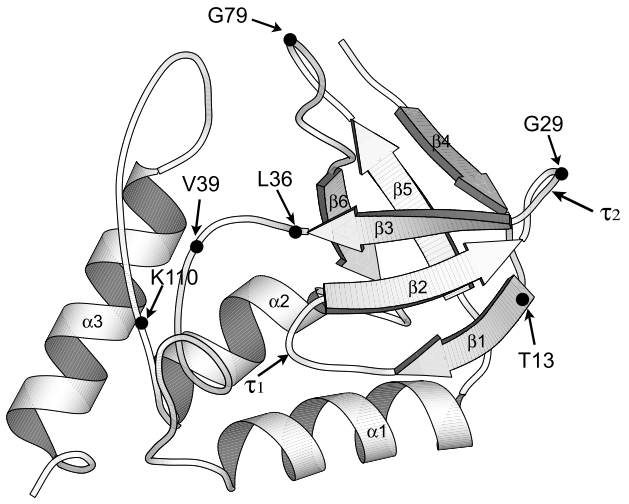

Fig. 1. Molscript representation of native SNase structure [16] (PDB entry 1STN). The regular secondary structures of six β-strands (β_1, β_2, β_3, β_4, β_5, and β_6), and two β-turns (τ_1 and τ_2) and three helices (α_1, α_2, and α_3) are indicated. The truncated sites and residues T13, G29, and V39 are labelled by residue number.

for G88W- and V66W-mutant of SNase110 to adopt a stable folded conformation [3,4]. The G88W mutant of SNase110 (G88W110) can self-associate to form soluble aggregates in the presence of 4.0 M urea [5]. However, no soluble aggregates can be detected in SNase36. As demonstrated before, the self-association reaction is correlated with residual β-structure in partially folded and denatured proteins [6,7]. Therefore, questions whether SNase79 undergoes aggregation and whether SNase79 takes some native-like conformation aroused our interest.

In this study, circular dichroism (CD), size-exclusion chromatography, and heteronuclear NMR spectroscopy were used to explore aggregation and folding features of SNase79 in aqueous solution. The results lead to a novel finding that the *cis*/*trans* heterogeneity of Gln30-Pro31 peptide bond influences the folding conformations and self-association reaction of SNase79 in aqueous solution.

Materials and methods

Protein expression and purification. The plasmid constructions for SNase79 and proline-free SNase79 ([Pro$^-$]SNase79) were achieved by polymerase chain reaction (PCR) of the genes of wild-type SNase and of [Pro$^-$]SNase (P11A/P31A/P42A/P47T/P56A/P117G / mutant of SNase), respectively. The PCR products were inserted into the *Nde*I and *Bam*HI sites of plasmid pET-3a, and were sequenced to confirm the presence of the desired mutations. All genes were cloned in plasmid pET-3a and expressed in the BL21 (DE3) strain of *Escherichia coli*. Protein expression was induced in LB culture with 0.4 mM isopropyl-1-thio-β-D-galactopyranoside (IPTG) when the $A_{600\,nm}$ of the culture reached a value of 1.0. After an additional incubation for 5 h at 37 °C, the cells were collected by centrifugation, suspended in lysis buffer, and purified as described by Ye et al. [3].

Uniformly ^{15}N- and ^{15}N/^{13}C-labelled fragments were obtained through bacterial growth in M9 minimal media using $^{15}NH_4Cl$ and [^{13}C]glucose as the sole ^{15}N and ^{13}C sources. The purity of proteins was checked by SDS–PAGE to ensure a single band.

Far-UV CD spectroscopy. Far-UV CD experiments were performed on SNase79 with concentrations of 15, 30, 50, and 100 μM in 25 mM Tris–HCl buffer (pH 7.0) on a Jasco 720 spectropolarimeter at room temperature. Measurements were acquired with 1 mm path length over the range of 190–240 nm. Four scans were averaged for each measurement.

Size-exclusion chromatography. Size-exclusion chromatography of SNase79 was carried out on a Superdex 75-HR gel filtration column (10×30 mm) interfaced with an AKTA fast performance liquid chromatography (FPLC) system (Amersham-Pharmacia Biotech). The effluent of each sample was monitored by measuring absorbance at 280 nm. Five SNase79 samples were prepared by dissolving the protein in buffer (100 mM Tris–HCl, pH 7.0) to the final concentrations of 50, 100, 250, 500, and 1000 μM. Each sample (200 μl) was injected into the column equilibrated with the elution buffer identical to the sample buffer. The chromatography was performed with a flow-rate of 0.5 ml/min at room temperature.

The molecular sizes of SNase79 at different protein concentrations can be depicted by determining their Stokes radii via measuring their elution volumes. The relation between Stokes radius (R_s) and the rate of elution ($1000/V_e$) is described by the following equation:

$$R_s = a + 1000b/V_e,$$

where V_e (ml) is the elution volume, and a and b are parameters that were determined by measuring the elution volumes of four standard proteins whose Stokes radii are known [8]. The determined a and b are -24.27 ± 1.41 and 0.5157 ± 0.014, respectively (Table 1).

NMR spectroscopy. All NMR experiments were carried out at 300 K on a Bruker DMX 600 spectrometer equipped with a triple-resonance cryo-probe. The 3D ^1H_N–^{13}C–^{15}N HNCA, HN(CO)CA, HNCACB, and CBCACONH were performed on SNase79 samples for backbone resonance assignments. 500 μM SNase79 in 90% H_2O/10% D_2O containing 20 mM d_4-acetate buffer (pH 4.9) was used for 3D HNCA and HN(CO)CA experiments. A sample of 400 μM SNase79 in the presence of 6.0 M urea was used for 3D HNCA, HN(CO)CA, HNCACB, and CBCACONH experiments. The 2D ^1H_N–^{15}N HSQC spectra were collected for a series of samples containing 5, 15, 50, 100, 200, 500, and 1000 μM SNase79 in aqueous solution. The 2D ^1H_N–^{15}N HSQC experiments were also run with [Pro$^-$]SNase79 at concentrations of 15 and 500 μM. The ^1H_N–^{15}N heteronuclear chemical exchange experiments were carried out on 400 μM SNase79 in 2.0 M urea with exchange delays of 12, 52, 102, 202, 402, 602, 802, 1002, 1202, 1402, 1602, 1802, and 2002 ms at 300 K [9]. All NMR data were processed and analyzed using FELIX98 (MSI/Accelrys). The data points in each indirect dimension were usually doubled by linear prediction before zero filling to the appropriate size. ^{1}H chemical shifts were referenced to that of internal 2,2-dimethyl-2-silapentane-5-sulfonate (DSS) at 0 ppm. ^{15}N and ^{13}C chemical shifts were referenced indirectly [10].

Table 1
Parameters of standard proteins for size exclusion column Superdex-75

Standard proteins	Elution volume (ml)	Molecular weight (kDa)	Stokes radius[a] (Å)
Ribonuclease	12.59	13.7	16.4
Chymotrysinogen	11.53	25.7	20.9
Ovalbumin	9.46	43	30
BSA	8.64	67	35.5

[a] Stokes radii are provided by Amersham-Pharmacia Biotech.

Results

Non-ordered conformation of SNase79

Fig. 2 provides far-UV CD spectra of SNase79 in aqueous solution. The CD spectra show a pronounced minimum around 200 nm and a shallow minimum at 220 nm, respectively. No significant change in the CD spectra was found at 50 μM SNase79 compared with those obtained for SNase79 at concentrations of 15 and 30 μM. However, dramatic changes in the CD spectrum were observed for 100 μM SNase79. This indicates that serious aggregation may occur for SNase79 at a concentration higher than 100 μM. The pattern of CD spectra in Fig. 2 reveals that molecules of SNase79 adopt mainly a non-ordered conformation which is responsible for the pronounced minimum around 200 nm. However, the shallow minimum at about 220 nm suggests the existence of some residual structure in SNase79.

Self-association reaction of SNase79

The size exclusion chromatography profiles for SNase79 at protein concentrations of 50, 100, 250, 500, and 1000 μM are shown in Fig. 3. One main elution peak was obtained for each SNase79 sample. SNase79 of different concentrations eluted at different elution volumes. A trend of decreasing elution volume (V_e) of main elution peak was observed while the concentration of SNase79 was increased from 50 to 1000 μM. Since a small amount of SNase79 was used for each sample injected into the column (the highest amount of SNase79 was about 2.2 mg for a protein concentration of 1000 μM), the concentration effect on the elution profile can be excluded. Therefore, the main elution peaks can be used to determine the Stokes radii of SNase79 at different concentrations. The measured elution volumes and the calculated Stokes radii for SNase79 at different concentrations are listed in Table 2. It can be seen that the elution volume and Stokes radius decrease and increase, respectively, with increasing the protein concentration. This indicates that an increase in the protein concentration can convert SNase79 into soluble aggregates. As previously reported, the exposed hydrophobic surface of the β-structures is prone to self-association reaction in proteins [6,7]. SNR79, an analogue of SNase79, in which a hexapeptide is appended to the N-terminal of SNase79, showed a certain amount of residual β-strands and turns [11]. Therefore, SNase79 may self-associate in aqueous solution and the main elution peaks represent the fraction of SNase79 at certain aggregated states.

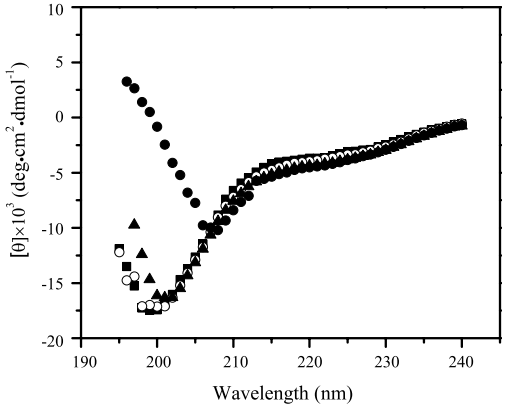

Fig. 2. Far-UV CD spectra of SNase79 at concentrations of 15 μM (■); 30 μM (○); 50 μM (▲); and 100 μM (●).

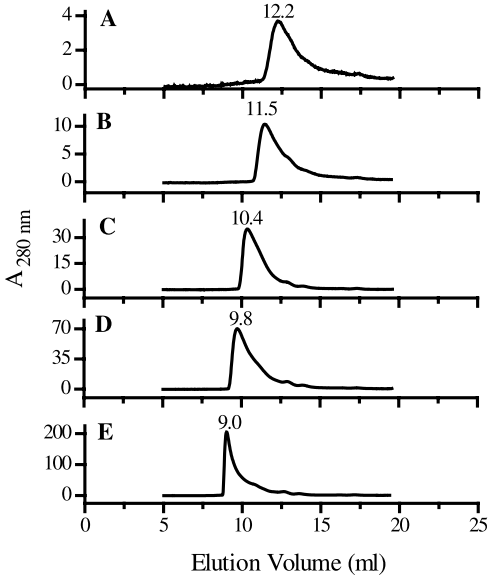

Fig. 3. Elution profiles obtained on SNase79 at different concentrations: 50 μM (A), 100 μM (B), 250 μM (C), 500 μM (D), and 1000 μM (E).

Cis/trans heterogeneity-related doubling of NMR peaks

The backbone $^{1}H_N$ and ^{15}N resonances of SNase79 at 500 μM in aqueous solution and SNase79 at 400 μM in 6.0 M urea were assigned by analysis of the 3D heteronuclear NMR spectra. The $^{1}H_N$–^{15}N cross-peaks in the 2D HSQC spectra of SNase79 at different concentrations showed very small changes in the chemical shifts.

Table 2
Elution volumes and Stokes radii obtained for SNase79 at different concentrations

Concentration (M)	Elution volume (ml)	Stokes radius (Å)
50	12.2	18.35
100	11.5	20.95
250	10.4	25.73
500	9.8	28.79
1000	9.0	33.51

Therefore, the backbone $^{1}H_N$ and ^{15}N resonances in the HSQC spectra of SNase79 at high concentrations were assigned based on the similarity of chemical shifts to the corresponding resonances in the spectrum of SNase79 at 500 μM. The assignments of cross-peaks in the HSQC spectra of SNase79 at low concentrations were achieved by comparison with the spectrum of SNase79 at 400 μM in 6.0 M urea. In Fig. 4A, the assigned $^{1}H_N$–^{15}N cross-peaks are indicated with the one-letter amino acid code and residue number in the 2D $^{1}H_N$–^{15}N HSQC spectrum of 50 μM SNase79.

Several residues of SNase79 show two sets of cross-peaks with unequal intensities in the 2D $^{1}H_N$–^{15}N HSQC spectrum (Fig. 4A). Among these residues are Glu10, Gly29, and Gly55. Each of these residues generates a major cross-peak with high signal intensity and a minor cross-peak with low signal intensity in the NMR spectrum. No exchange cross-peaks could be observed between the two sets of cross-peaks for these residues in the $^{1}H_N$–^{15}N heteronuclear chemical exchange spectra acquired with 400 μM SNase79 in 2.0 M urea. Thus, the exchange between the major and minor cross-peaks of these residues is very slow in SNase79.

SNase79 contains five prolines at positions 11, 31, 42, 47, and 56 in sequence. Peptide bonds of Glu10-Pro11, Gln30-Pro31, and Thr41-Pro42 are in the *trans*-conformation and peptide bond of Gly55-Pro56 is in the *cis*-conformation in the native SNase [12,13]. The prolyl *cis*/*trans* isomerization of His46-Pro47 peptide bond was observed for the native SNase. Gly29 is located in the β-turn τ_2 (Tyr27-Lys28-Gly29-Gln30) of the native SNase (the cross-peak of Gln30 is in a crowded region of the HSQC spectrum, so that its minor cross-peak is difficult to identify). In the $^{1}H_N$–^{15}N 2D HSQC spectrum of the proline-free SNase79, a single set of signals was observed for these residues (Fig. 4B). Therefore, doubling of the cross-peaks for these residues is considered as the result of *cis*/*trans* heterogeneity at the X-prolyl peptide bonds of SNase79.

Conformational heterogeneity of SNase79

The 2D $^{1}H_N$–^{15}N HSQC experiments were carried out on SNase79 samples of various protein concentrations ranging from 5 to 1000 μM. The concentration-dependent aggregation of SNase79 influences the line width of resonance signals in NMR spectra. A pronounced decrease in intensity of $^{1}H_N$–^{15}N cross-peaks in the 2D $^{1}H_N$–^{15}N HSQC spectra of SNase79 while increasing the protein concentration was observed for residues, Thr13, Leu14, Lys16, Ala17, Ile18, Gly20, Asp21, Thr22, Val23, Gly29, Gln30, Met32, Thr33, and Val39. However, the cross-peaks for residues in the sequence regions other than Thr13-Val39 and all the minor cross-peaks did not show any decrease in intensity even at high protein concentration of 1000 μM (Fig. 5). Fig. 6 shows the concentration-depen-

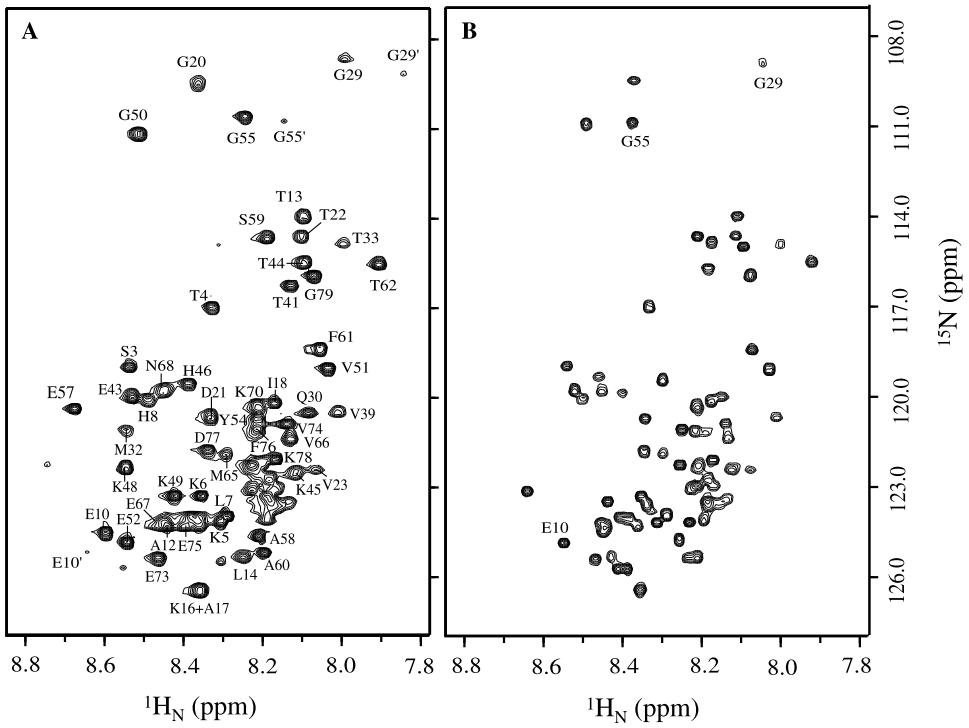

Fig. 4. 2D $^{1}H_N$–^{15}N HSQC spectra of 50 μM SNase79 (A) and 15 μM [Pro$^-$]SNase79 (B) in aqueous solution. The assigned cross-peaks are indicated for 50 μM SNase79 and the minor cross-peaks observed for 50 μM SNase79 are denoted in (A).

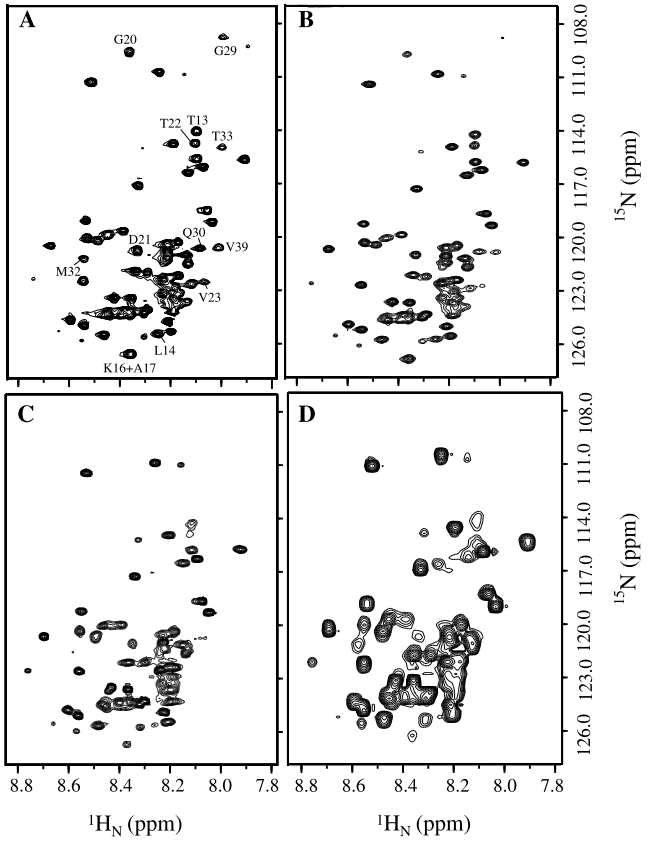

Fig. 5. 2D $^{1}H_N$–^{15}N HSQC spectra of SNase79 at different concentrations: 50 μM (A), 100 μM (B), 500 μM (C), and 1000 μM (D).

dence of the major and minor cross-peaks for residues Glu10, Gly29, and Gly55. The concentration-dependence was described by the intensity ratio of cross-peaks for these three residues to cross-peak of Gly79, since Gly79 is at the C-terminus of SNase79. The major cross-peak of Gly29 shows a strong concentration-dependence, and it illustrates the decrease in $^{1}H_N$–^{15}N HSQC cross-peak intensities of residues Thr13-Val39 accompanying the protein aggregation. In contrast, the concentration-dependence of the intensity of the minor cross-peak of Gly29 is very weak. Notable exceptions are residues Glu10 and Gly55 which show very weak concentration-dependence of both major and minor cross-peak intensities. The data illustrated in Fig. 6 suggest that the great population of SNase79 generating the major cross-peak of Gly29 is involved in self-association reaction and the minor cross-peak of Gly29 corresponds to a small population of SNase79 which is precluded from aggregation and is essentially in a monomeric state. Both self-associated SNase79 and monomeric SNase79 provide the major and minor cross-peaks for Glu10 and Gly55 and other residues. The segment Thr13-Val39 of the monomeric and self-associated SNase79 has different conformations. Therefore, an ensemble of highly heterogeneous conformations is observed for SNase79 in aqueous solution.

Discussion

Far-UV CD spectra, size-exclusion chromatography, and NMR studies on SNase79 demonstrated that SNase79 undergoes self-association reaction and that sequence region Thr13-Val39 (Fig. 1) is responsible for association interface of SNase79. The segment Thr13-Val39 encompasses all the amino acid residues forming the β-sheet (βI) of native SNase, and Gly29 is located in the β-turn τ_2 linking two β-strands in β-sheet (βI). A previous study reported that the association-induced line-broadening effects were observed for large SNase fragments containing residual β-sheet structure [5]. An NMR investigation of self-association reactions indicated that β-strands predominate in association interface of the protein [7]. Therefore, the concentration-dependence of the major cross-peak intensity of Gly29 characterizes the conformation of highly populated SNase79, in which the segment Thr13-Val39 may adopt a native-like β-sheet conformation. The minor cross-peak of Gly29 corresponds to the species of SNase79 having non-native conformation and the conformation of the segment Thr13-Val39 in the monomeric SNase79 may preclude SNase79 from

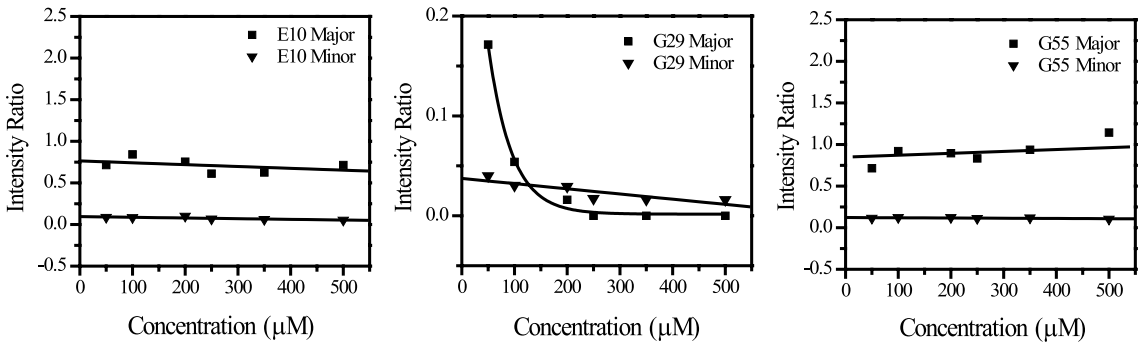

Fig. 6. Signal intensity of the major and minor cross-peaks of residues Glu10, Gly29, and Gly55 as a function of protein concentration. The signal intensity is described by the intensity ratio of these cross-peaks to cross-peak Gly29.

aggregation. This conformational heterogeneity is supposed to be correlated with the *cis*/*trans* heterogeneity of Gln30-Pro31 peptide bond in SNase79.

SNase79 is regarded as a SNase fragment in denatured state, the isomerization of X-prolyl bonds of Glu10-Pro11, Gln30-Pro31, and Gly55-Pro56 being observed in SNase79. However, all these three X-prolyl bonds show the stable isomers in the native SNase. The major and minor cross-peaks for the isomerization of these three peptide bonds are supposed to report the correct isomer (same to native isomer) and the wrong isomer (different from native isomer), respectively, with reference to the native case of the corresponding bonds. The exchange between two isomers of X-prolyl bonds in SNase79 is very slow with a lifetime longer than 2.0 s. Therefore, the multiple conformations are observed for SNase79. The major cross-peak of Gly29 is supposed to represent the correct *trans*-conformation of Gln30-Pro31 peptide bond, since it is correlated to the self-associated SNase79. The minor cross-peak of SNase79 is an indicator of the *cis*-conformation of Gln30-Pro31 peptide bond in the monomeric SNase79. The *cis*-conformation of Gln30-Pro31 peptide bond may influence the formation of β-sheet (βI) structure in the native SNase, and thus preclude SNase79 from self-association. This is confirmed by the observation of self-association reaction for [Pro^{-}]SNase79 which has *trans*-peptide bond of Gln30-Pro31 (data not shown).

It was suggested that the isomerization reaction toward the correct X-prolyl peptide conformation occurs before the folding of the protein to the native conformation. The wrong isomer of the peptidyl-proline bonds may cause protein folding to a misfolded intermediate [14]. This provides a basis to make an inference that the correct and the wrong X-prolyl peptide conformations of Gln30-Pro31 may have a different effect on the folding of SNase79. Nucleation–condensation mechanisms in protein folding refer the nucleus as the native-like secondary structure formed by neighboring residues and suggest that nucleation and overall structure formation are concerted [15]. The segment Tyr27-Gln30, forming a β-turn in the native SNase, is considered as the folding nucleation site of SNase fragments of different chain lengths starting from the N-terminal end [2]. Therefore, the native-like β-sheet conformation of the segment Thr13-Val39 in the large population of SNase79 deduced from the self-association reaction is coupled with nucleation at Tyr27-Gln30. The major cross-peak of Gly29 is an indicator for nucleation in the folding of SNase79, but this is not the case for the minor cross-peak of Gly29 of SNase79. In consequence, the *trans*-conformation of Gln30-Pro31 peptide bond responses for the native-like folding of the segment Thr13-Val39 in SNase79 and the *cis*-conformation of Gln30-Pro31 peptide bond cause SNase79 to be in an unfolded state. This determines whether SNase79 is able to undergo the self-association reaction in aqueous solution.

Acknowledgments

We thank Professor K. Kuwajima (University of Tokyo) for providing the plasmid of proline-free staphylococcal nuclease. This research was supported by the National Natural Science Foundation of China (NNSFC 39823001) and partially by NNSFC 30170201.

References

[1] J. Wang, D.M. Truckses, F. Abildgaard, Z. Dzakula, Z. Zolnai, J.L. Markley, Solution structures of staphylococcal nuclease from multidimensional, multinuclear NMR: nuclease-H124L and its ternary complex with Ca^{2+} and thymidine-3′,5′-bisphosphate, J. Biomol. NMR 10 (1997) 143–164.

[2] J. Dai, X. Wang, Y. Feng, G. Fan, J. Wang, Searching for folding initiation sites of staphylococcal nuclease: a study of N-terminal short fragments, Biopolymers 75 (2004) 229–241.

[3] K. Ye, G. Jing, J. Wang, Interactions between subdomains in the partially folded state of staphylococcal nuclease, Biochim. Biophys. Acta 1479 (2000) 123–134.

[4] Y. Feng, D. Liu, J. Wang, Native-like partially folded conformations and folding process revealed in the N-terminal large fragments of staphylococcal nuclease: a study by NMR spectroscopy, J. Mol. Biol. 330 (2003) 821–837.

[5] K. Ye, J. Wang, Self-association reaction of denatured staphylococcal nuclease fragments characterized by heteronuclear NMR, J. Mol. Biol. 307 (2001) 309–322.

[6] A.T. Alexandrescu, F.P. Lamour, V.A. Jaravine, NMR evidence for progressive stabilization of native-like structure upon aggregation of acid-denatured LysN, J. Mol. Biol. 295 (2000) 239–255.

[7] A.T. Alexandrescu, K. Rathgeb-Szabo, An NMR investigation of solution aggregation reactions preceding the misassembly of acid-denatured cold shock protein A into fibrils, J. Mol. Biol. 291 (1999) 1191–1206.

[8] V.N. Uversky, Use of fast protein size-exclusion liquid chromatography to study the unfolding of proteins which denature through the molten globule, Biochemistry 32 (1993) 13288–13298.

[9] N.A. Farrow, O. Zhang, J.D. Forman-Kay, L.E. Kay, A heteronuclear correlation experiment for simultaneous determination of 15N longitudinal decay and chemical exchange rates of systems in slow equilibrium, J. Biomol. NMR 4 (1994) 727–734.

[10] J.L. Markley, A. Bax, Y. Arata, C.W. Hilbers, R. Kaptein, B.D. Sykes, P.E. Wright, K. Wuthrich, Recommendations for the presentation of NMR structures of proteins and nucleic acids. IUPAC-IUBMB-IUPAB inter-union task group on the standardization of data bases of protein and nucleic acid structures determined by NMR spectroscopy, J. Biomol. NMR 12 (1998) 1–23.

[11] K. Tian, B. Zhou, F. Geng, G. Jing, Folding of SNase R begins early during synthesis: the conformational feature of two short N-terminal fragments of staphylococcal nuclease R, Int. J. Biol. Macromol. 23 (1998) 199–206.

[12] J.F. Wang, A.P. Hinck, S.N. Loh, J.L. Markley, Two-dimensional NMR studies of staphylococcal nuclease. 2. Sequence-specific assignments of carbon-13 and nitrogen-15 signals from the nuclease H124L-thymidine 3′,5′-bisphosphate-Ca^{2+} ternary complex, Biochemistry 29 (1990) 102–113.

[13] S.N. Loh, C.W. McNemar, J.L. Markley, Detection and kinetic characterization of a novel proline isomerism in staphylococcal nuclease by NMR spectroscopy, in: J. Villafranca (Ed.), Techniques in Protein Chemistry II, Academic Press, New York, 1991, pp. 275–282.
[14] Y.J. Tan, M. Oliveberg, D.E. Otzen, A.R. Fersht, The rate of isomerisation of peptidyl–proline bonds as a probe for interactions in the physiological denatured state of chymotrypsin inhibitor 2, J. Mol. Biol. 269 (1997) 611–622.
[15] A.R. Fersht, Nucleation mechanisms in protein folding, Curr. Opin. Struct. Biol. 7 (1997) 3–9.
[16] T.R. Hynes, R.O. Fox, The crystal structure of staphylococcal nuclease refined at 1.7 A resolution, Proteins 10 (1991) 92–105.